Brain Structure and Function (2019) 224:1659–1676
https://doi.org/10.1007/s00429-019-01865-1

ORIGINAL ARTICLE

Ventral midline thalamus lesion prevents persistence of new (learning-triggered) hippocampal spines, delayed neocortical spinogenesis, and spatial memory durability

Marie Muguet Klein[1,2] · Thibault Cholvin[1,2] · Brigitte Cosquer[1,2] · Aurélie Salvadori[1,2] · Julia Le Mero[1,2] · Lola Kourouma[1,2] · Anne-Laurence Boutillier[1,2] · Anne Pereira de Vasconcelos[1,2] · Jean-Christophe Cassel[1,2]

Received: 13 December 2018 / Accepted: 20 March 2019 / Published online: 29 March 2019

Abstract

The ventral midline thalamus contributes to hippocampo-cortical interactions supporting systems-level consolidation of memories. Recent hippocampus-dependent memories rely on hippocampal connectivity remodeling. Remote memories are underpinned by neocortical connectivity remodeling. After a ventral midline thalamus lesion, recent spatial memories are formed normally but do not last. Why these memories do not endure after the lesion is unknown. We hypothesized that a lesion could interfere with hippocampal and/or neocortical connectivity remodeling. To test this hypothesis, in a first experiment male rats were subjected to lesion of the reuniens and rhomboid (ReRh) nuclei, trained in a water maze, and tested in a probe trial 5 or 25 days post-acquisition. Dendritic spines were counted in the dorsal hippocampus and medial prefrontal cortex. Spatial learning resulted in a significant increase of mushroom spines in region CA1. This modification persisted between 5 and 25 days post-acquisition in Sham rats, not in rats with ReRh lesion. Furthermore, 25 days after acquisition, the number of mushroom spines in the anterior cingulate cortex (ACC) had undergone a dramatic increase in Sham rats; ReRh lesion prevented this gain. In a second experiment, the increase of c-Fos expression in CA1 accompanying memory retrieval was not affected by the lesion, be it for recent or remote memory. However, in the ACC, the lesion had reduced the retrieval-triggered c-Fos expression observed 25 days post-acquisition. These observations suggest that a ReRh lesion might disrupt spatial remote memory formation by preventing persistence of early remodeled hippocampal connectivity, and spinogenesis in the ACC.

Keywords Anterior cingulate cortex · c-Fos imaging · Dendritic spines · Golgi staining · Hippocampus · Medial prefrontal cortex · Rat · Spatial memory · Systems-level consolidation

Introduction

Declarative memories in humans and declarative-like ones in other animals become enduring over a consolidation process known as systems consolidation (e.g., Frankland and Bontempi 2005; Squire et al. 2015). Closely after encoding, which requires an engagement of prefrontal cortical regions (e.g., Squire et al. 2015), a still labile memory trace is stored in and retrieved from hippocampal modules. Over time, the hippocampus (Hip) triggers a reorganization of this memory within previously tagged neocortical modules (Lesburgueres et al. 2011), whereby the memory becomes robust, lasting, and possibly independent of the Hip (Frankland and Bontempi 2005; Squire et al. 2015). Systems consolidation is orchestrated by a functional dialog between the Hip and the medial prefrontal cortex (mPFC), in which the information can travel monosynaptically from the former to the latter (e.g., Thierry et al. 2000), but requires a relay on the way back to the Hip. Indeed, monosynaptic projections have not been described in this direction (e.g., Vertes 2004). One such relay could

Marie Muguet Klein, Thibault Cholvin, Anne Pereira de Vasconcelos, Jean-Christophe Cassel share an equivalent contribution to this manuscript.

✉ Jean-Christophe Cassel
jcassel@unistra.fr

[1] Laboratoire de Neurosciences Cognitives et Adaptatives (LNCA), UMR 7364, Université de Strasbourg-CNRS, 12 rue Goethe, 67000 Strasbourg, France

[2] CNRS, LNCA UMR 7364, 67000 Strasbourg, France

be constituted by the reuniens (Re) and rhomboid (Rh) nuclei. These two ventral midline thalamic nuclei have reciprocal connections with the Hip and mPFC (Cassel et al. 2013). Some Re neurons even have collaterals projecting to both structures (Hoover and Vertes 2012; Varela et al. 2014). It is also worth mentioning that communication from the Hip to the mPFC occurs at theta frequency via direct projections, whereas communication from the mPFC to the Hip occurs at 2–5 Hz frequencies in the delta band through a relay in the Re (Roy et al. 2017).

Data in the literature indicate that ReRh nuclei have crucial implications in cognitive processes, especially in tasks requiring a coordinated activation of the Hip and mPFC (e.g., Cassel et al. 2013). For instance, these nuclei take part in the generalization of fear memory attributes (Xu and Südhof 2013), in strategy shifting (Cholvin et al. 2013), and in spatial working memory tasks (Griffin 2015). Hallock et al. (2016) showed in a T-maze that correct spatial working memory performance required a Re-dependent modulation of Hip-mPFC synchrony. Regarding systems consolidation, Loureiro et al. (2012) found that the ReRh of intact rats exhibited a strong increase of c-Fos expression when the animals had to retrieve a remote spatial memory, not when they retrieved a recent one. Furthermore, following fiber-sparing lesion of the ReRh, rats learned a Morris water maze task normally, showed intact performance in a probe trial taxing recent memory (at 5 days post-acquisition), but were dramatically impaired when the probe trial assessed remote memory (at 25 days post-acquisition; Loureiro et al. 2012). Loureiro et al. also found that reversible inactivation of the ReRh nuclei altered neither recent nor remote memory retrieval, suggesting that it is the systems consolidation process that the lesion disrupted, not the remote memory retrieval process. Interestingly, the region encompassing the ReRh could also contribute to remote memory processing in humans (Thielen et al. 2015).

Using contextual fear conditioning, hence a task requiring the Hip, Restivo et al. (2009) investigated synaptic rearrangements related to systems consolidation in the Hip and mPFC of mice. They found that the number of dendritic spines was increased in the Hip, but not in the mPFC at a short post-conditioning delay (1 day), and that an almost opposite picture was observed after a longer delay (30 days). From the aforementioned observations, we hypothesized that if a ReRh lesion affected systems-level consolidation of spatial memories, we should find (i) differences in spine density within the Hip and the mPFC between short (5 days) and long (25 days) delays after acquisition of a Morris water maze (WM) task, (ii) prevention by ReRh lesion of these changes at a remote but not a recent time point, and (iii) an absence of retrieval-related modifications of c-Fos expression in the mPFC during remote memory testing in rats with a ReRh lesion.

Materials and methods

In the first experiment, we used Golgi staining to investigate the consequences of a ReRh lesion on baseline (no learning) and recent vs. remote memory formation-triggered changes in dendritic spine densities in the dorsal Hip (dHip, CA1, CA3, and dentate gyrus) and mPFC (anterior cingulate, infralimbic, and prelimbic cortices). In the second experiment, using c-Fos immunostaining, we checked in intact rats if the brain regions in which the dendritic spine densities had undergone modifications were activated during recent vs. remote memory retrieval, and whether the activation pattern was altered by the ReRh lesion.

Subjects

The study conformed to the rules of the European Community council directive of 22 September 2010 (2010-63) and of the French Department of Agriculture. All approaches have been validated by a local ethical committee (CREMEAS—authorization no. AL/32/39/02/13). The first and second experiments used 95 and 75 male Long-Evans rats, respectively. These animals were 3 months old and weighted 250–280 g at their arrival in the laboratory. They were housed in quiet facilities under a 12 h light/dark cycle (light on at 7:00 A.M.) with ad libitum access to food and water, controlled temperature (~ 23 °C), and a hygrometry of about 55%. All rats were kept under these conditions for the whole duration of the experiment. Animals were individually handled for 2–3 min each day over 5 consecutive days before surgery, and again before maze training. Part of them were trained and tested in a water-maze task. The others were kept in their home cage (HC) as controls for Golgi-Cox staining (Experiment 1) and c-Fos expression (Experiment 2).

Surgical procedure: fiber-sparing excitotoxic lesion

Surgeries were conducted under aseptic conditions as previously described (Cholvin et al. 2013; Loureiro et al. 2012). Rats were anesthetized with sodium pentobarbital (50 mg/kg, i.p.) and secured in a stereotaxic frame (incisor bar: − 3 mm). Excitotoxic fiber-sparing lesion targeting the ventral midline thalamus (ReRh) was made using slow microinfusions of 0.1 M *N*-methyl-D-aspartate (NMDA: 0.1 µL/site over 2 min, dissolved in phosphate-buffered saline; Sigma- Aldrich) via an infusion needle (0.28 mm in diameter) connected to a motorized infusion pump (CMA 100). After leaving the needle in situ for an additional 5 min to ensure diffusion of NMDA into the target structure, it was slowly retracted. The three infusion sites had the following coordinates (in mm): AP = − 1.5, − 2.1 and

− 2.7 mm (from bregma, respectively), DV = − 7.0, − 7.1 and − 7.2 mm (from skull, respectively), ML = + 1.8, + 1.8 and + 1.9 mm (from midline of the sagittal sinus, respectively). All coordinates are given according to Paxinos and Watson (2007). We used a ML angle of 15°. The sham-operated controls (Sham) were infused with an equivalent volume of phosphate-buffered saline at exactly the same coordinates. After surgery, rats were allowed to recover under a warm lamp for 20–30 min before being placed back into their home cage, where they were given a two-week rest before the start of behavioral training.

Morris water-maze task

The water maze consisted of a circular pool (diameter 160 cm; height 60 cm) filled with water (21 ± 1 °C). Water was made opaque by the addition of powdered milk (about 1.5 g/L). The first day consisted in pretraining based on a unique 4-trial session with a visible platform (Fig. 1a). The platform had a diameter of 11 cm, was painted black and protruded 1 cm above the water surface. It was located in the South–East quadrant of the pool. The rats were started randomly from four different locations at the edge of the pool. During pretraining, a blue curtain surrounded the pool to prevent the use of distal cues, and thus incidental encoding of spatial information. This pretraining session facilitates subsequent acquisition of the hidden platform task, rats having already learned that there was an escape platform in the pool. On the next day, the curtain was removed. Rats were then given an 8-day training with four successive acquisition trials per day (intertrial interval, 10–15 s) of a maximum duration of 60 s to learn a new location of the platform, now hidden 1 cm below the water surface (in the North–West quadrant, Fig. 1a). The sequence of the four different start locations was randomized on each day. During acquisition, a video-tracking system (SMART; PanLab) recorded the distance travelled, average swim speed, latency before reaching the platform, as well as thigmotactic behavior (i.e., time spent swimming along the edge of the pool). For the probe trial, the platform was removed. The rats were introduced in the pool from a start point never used previously (the North–East) and allowed a 60-s swimming time to explore the pool. The time spent in the target quadrant (i.e., where the platform was located during acquisition), the number of crossings above the annulus (corresponding to the surface of the platform enlarged by a 10-cm wide annulus) used as an index of memory precision (e.g., Lopez et al. 2012), as well as the latency to reach the former platform location were recorded. Thigmotactic behavior and average swim speed were also collected.

Experiment 1: Effects of learning and ReRh lesion on structural plasticity in the dorsal hippocampus and mPFC

NeuN immunohistochemistry to check for the placement and extent of the lesion

Brain preparation and sectioning

Immediately after the water-maze probe test, rats were deeply anesthetized with an overdose of pentobarbital (200 mg/kg i.p.). Home cage rats were killed the same way at the same time. The brains were quickly removed and dissected in three parts: a block of tissue containing the reuniens and rhomboid nuclei was removed with a razor blader and dipped for 4 h in a solution of paraformaldehyde in 0.1 M PBS (4%, 4 °C). This block was then transferred to a 20% sucrose solution (in 0.1 M PBS) for 48 h at 4 °C, before being snap-frozen in isopentane (− 40 °C, 1 min) and stored at − 80 °C until sectioning. Free-floating coronal Sects. (40 µm) were cut serially in a cryostat (Microm, HS 500) and stored in cryoprotectant at − 20 °C before being processed for immunostaining. The two other tissue blocks were used for Golgi cox staining. One extending from + 4.00 to + 2.52 mm from Bregma encompassed the mPFC. The other, between − 1.20 mm and − 4.36 mm from Bregma, encompassed the dHip (coordinates according to Paxinos and Watson 2007).

Immunohistochemistry protocol

NeuN immunochemistry was performed using a mouse anti-NeuN antibody (1:2000, ref MAB377; Millipore) as the primary antibody, and a biotinylated anti-mouse horse antibody (1:500; Vector Laboratories) as the secondary antibody. The protocol is described in Loureiro et al. (2012). Briefly, sections were rinsed three times during 10 min in a PBS merthiolate buffer before being soaked for 1 h in 5% normal donkey serum in PBS containing 0.5% Triton X-100. The sections were subsequently transferred into the primary anti NeuN antibody solution for 18 h at room temperature. Then, they were soaked in a buffer solution containing the secondary antibody. Staining was performed with the avidin–biotin–peroxidase method (Vectastain ABC kit; Vector Laboratories) coupled to diaminobenzidine.

Evaluation of lesion placement and extent

Serial sections through the thalamic block stained for NeuN were used to visualize the lesion placement and extent (Fig. 1b). Lesions were drawn using the relevant plates of the

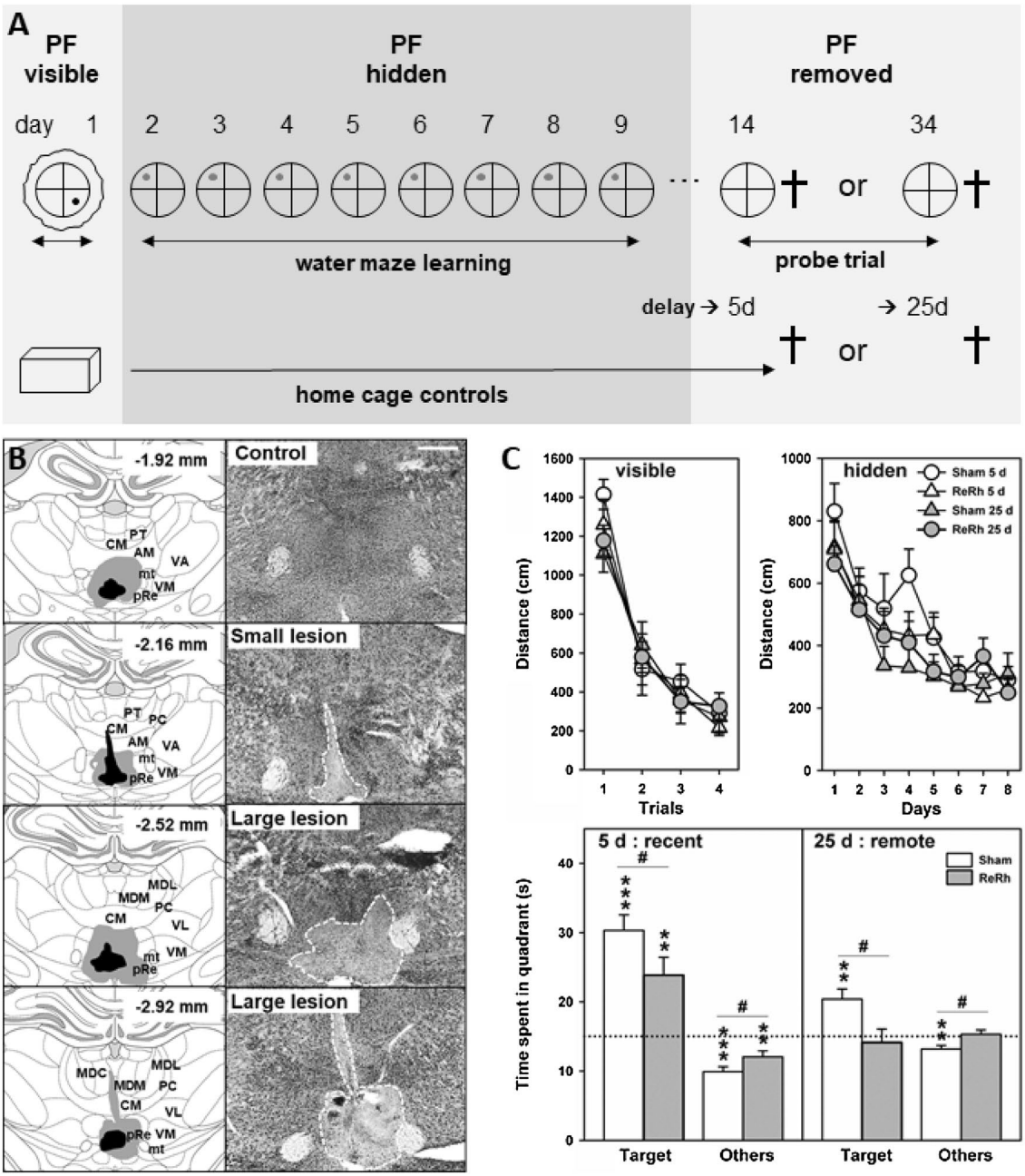

Fig. 1 **a** Timeline of behavioral testing in Experiment 1. Training started with the visible platform 2 weeks after lesion surgery. Recent memory was tested 5 days later and remote memory 25 days after the end of task acquisition, thus 14 and 34 days after visible platform (PF) pretraining, respectively. Experiment 2 used the same timeline. Rats were killed closely after the probe trial in both experiments. **b** Lesion size and location. Drawing of the smallest (dark gray) and largest (light gray) ReRh lesions on plates corresponding to coronal sections of the rat brain (left, anteroposterior level given in mm according to Paxinos and Watson 2007), and photomicrographs illustrating some typical small and large lesions (right) on brain sections immunostained for NeuN in Experiment 1. Scale bar = 1 mm. *AM* Anteromedial thalamic nucleus, *CM* central medial thalamic nucleus; *MDC* mediodorsal thalamic nucleus, central part, *MDM* mediodorsal thalamic nucleus, medial part, *mt* mammillothalamic tract, *PC* paracentral thalamic nucleus, *pRe* perireuniens thalamic nucleus, *PT* paratenial thalamic nucleus, *Sub* submedius thalamic nucleus, *VA* ventral anterior thalamic nucleus, *VL* ventrolateral thalamic nucleus, *VM* ventromedial thalamic nucleus. **c** Learning and memory performance in the water maze (WM) task. Performance of sham-operated rats (Sham) and of rats subjected to excitotoxic lesions of the reuniens and rhomboid nuclei (ReRh) in the WM task using a visible platform (visible), a hidden platform (hidden), and during the probe trial assessing recent memory at a post-acquisition delay of 5 days (5 day: recent) or remote memory at a post-acquisition delay of 25 days (25 days: remote). In rats with ReRh lesions, acquisition of the hidden platform task was normal, and rats remembered the platform location at the 5-day delay. Contrariwise, at the 25-day delay, only sham-operated rats were able to remember the platform location. Statistical analyses: significantly above chance level (dotted line): $^{**}p < 0.01$, $^{***}p < 0.001$; significant effect of the lesion: $^{\#}p < 0.05$

rat brain atlas (Paxinos and Watson 2007), from where they were replicated on electronic copies of the atlas. Automated pixel counts of the thalamic nuclei in the target regions and of their damaged part were used to estimate the lesion extent, including in regions adjacent to the ReRh. According to Groenewegen and Witter (2004), the Re nucleus is bordered by the so-called perireuniens (pRe). As the Re, the pRe has connections with limbic structures, particularly with the mPFC (Hoover and Vertes 2012). Acceptable lesions were defined as having damaged at least 50% of the Re nucleus and 25% of the Rh, with limited damage to the other adjacent thalamic regions. After the exclusion of animals ($n = 12$) displaying misplaced NMDA infusion sites or lesions of insufficient extent, the total number of rats in each experimental condition was as follow: 10 rats with ReRh lesions tested for recent memory, 9 rats with ReRh lesions tested for remote memory, 10 sham-operated rats per post-acquisition delay, 14 HC Sham rats for each delay, 7 HC rats with ReRh lesions for the short delay, and 9 other rats for the long delay. Half of the HC rats were killed at the same time as the rats of the 5-day post-acquisition delay, the other half were killed at the same time as the rats of the 25-day post-acquisition delay.

Golgi–Cox staining

Tissue preparation

The two tissue blocks including the mPFC and the hippocampus, respectively, were rinsed in bi-distilled water and immersed into impregnation solution made by mixing equal volumes of commercial solutions A (potassium dichromate and mercuric chloride) and B (potassium chromate) and stored for 3 weeks in darkness at room temperature. The blocks were then transferred into solution C, in which they were kept for 48 h in darkness, at 4 °C. The A, B and C reagents were from FD Neurotechnologies, Inc. Subsequently, coronal sections were cut at a thickness of 100 µm, still in darkness, using a vibratome, and mounted on gelatinized slides in solution C. The slides were dried, rinsed in bi-distilled water, stained in the staining solution, dehydrated in successive baths of ethanol, cleared in xylene, and coverslipped with Eukitt.

Quantification of dendritic spines

Spine density was measured on pyramidal neurons located in layers II/III of the anterior cingulate (ACC), prelimbic (PL) and infralimbic (IL) cortices, and in CA1, CA3, and dentate gyrus (DG) subfields of the dorsal hippocampus. These structures were defined according to the rat brain atlas (Paxinos and Watson 2007). For each hemisphere, three neurons were chosen in the counting window. To-be-analyzed neurons were selected under a light-transmission microscope (Leica DM550B) using low magnification. A neuron had to respond to three criteria to be selected for quantification, as in Restivo et al. (2009): (1) the dendrite had to be untruncated, (2) staining and impregnation had to be homogenous along the entire extent of the dendrite, and (3) neurons had to be easily discernible and relatively well isolated from neighboring impregnated cells. Measurements were performed on apical and basal dendrites in each region, at least 50 µm away from the soma for the apical dendrites, and at least 30 µm away for the basal dendrites, on secondary and tertiary branches. These distances allowed us to exclude dendritic segments near the soma that were essentially devoid of spines. For each neuron, six 20-µm long segments were randomly selected on apical and basal dendrites within a distance of at most 100 µm from the limit of the exclusion zone. Counting was performed under a 1000 × magnification using an oil immersion objective. Spines were counted blind to the experimental conditions. The density of spines was calculated for mushroom spines and, separately, for thin and stubby spines in a single category (Bourne and Harris 2007). The thin spine is identified as a protrusion of the membrane consisting in a small bulbous head and a thin and long neck. The stubby spine is defined as a relatively massive protrusion of the membrane lacking an apparent neck. Finally, the mushroom spine, as its name indicates, is a protrusion of the membrane made of a large mushroom-shaped (chanterelle-like) head. In the literature, mushroom spines have been considered mature, possibly supporting memory, whereas thin and stubby spines have been regarded as immature, possibly contributing to learning (e.g., Bourne and Harris 2007).

Experiment 2: Effects of ReRh lesion on neuronal activation in the hippocampus and mPFC after retrieval

NeuN immunohistochemistry to check for the placement and extent of the lesion

Brain preparation and section processing

90 min after the probe test in the water maze, rats received an overdose of pentobarbital (200 mg/kg i.p.) and were perfused transcardially with a 4% phosphate-buffered (0.1 M) paraformaldehyde (PFA, 4 °C) solution. Brains were removed, post-fixed for 4 h (4% PFA, 4 °C) and transferred to a 20% sucrose solution for 48 h at 4 °C before being snap-frozen (isopentane, − 40 °C, 1 min) and stored at − 80 °C. Free-floating coronal Sects. (40 µm) were cut in serial sections using a cryostat (Microm, HS 500). These sections were prepared from two tissue blocks including the mPFC and ReRh-dHip (the two latter

structures being partly overlaping in their antero-posterior extent), respectively (same extent as above). Home Cage (HC) animals were treated exactly the same way and at the same time. Starting at a random position, every sixth section was selected for NeuN immunohistochemistry and the following one for cresyl violet staining (for verification of the location and extent of the lesion). The next section was kept for c-Fos immunochemistry. Brain sections dedicated to cresyl violet staining were mounted onto gelatin-coated slides, stained and examined under light microscopy. All sections to be stained for c-Fos expression were collected and stored in cryoprotectant at − 20 °C before being processed.

Anti NeuN immunohistochemistry protocol

NeuN immunochemistry was performed exactly as described above (Experiment 1).

Evaluation of lesion placement and extent

Lesion verifications were performed exactly as for Experiment 1.

c-Fos immunohistochemistry protocol

After the exclusion of animals displaying misplaced NMDA infusion sites (n =10), the total number of rats was as follows: for rats with a ReRh lesion, recent memory (5day-Learn: n = 8; remote memory (25days-Learn): n = 8; home cage: n = 6 and 7 at the recent and remote time points (5d-HC and 25day-HC), respectively; for sham-operated rats, recent memory (5day-Learn): n =11; remote memory (25day-Learn): n =10; home cage: n = 8 and 7 at the recent and remote time points (5day-HC and 25day-HC), respectively. Sections dedicated to c-Fos immunochemistry were processed at the same time, whatever the group or the delay, with a balanced distribution in each of the 24-well boxes used for staining (including HC rats). These precautions minimized technical bias. The sections were first rinsed three times during 10 min in PBS before being soaked for 1 h in 5% normal donkey serum in PBS, subsequently transferred into the primary anti-Fos rabbit polyclonal antibody (1:4000, Rabbit anti-Fos polyclonal IgG; Santa Cruz, USA) solution for 18 h at room temperature, and then soaked in a buffer solution containing the biotinylated goat anti-rabbit secondary antibody (1:500, Biotin-SP-conjugated affiniPure Goat anti-rabbit IgG, Jackson ImmunoResearch, West Grove, PA, USA). Staining was revealed with avidin–biotin–peroxidase coupled with diaminobenzidine (Lopez et al. 2012).

Stereological analyses of c-Fos labelled sections

The quantitative analyses of c-Fos-positive nuclei were performed in the three mPFC subregions (ACC, PL, IL), as well as in the three dHip areas (CA1, CA3, DG). Quantifications were performed on eight sections per animal. A single investigator, blind to the rats' treatment, stereologically analyzed all specimens. The overall number of c Fos-immunoreactive neurons was counted using the optical fractionator technique allowing unbiased counting (West et al. 1991; West 2013). The image analyses system consisted of a Leica DM5500B light microscope equipped with a motorized x–y stage control and coupled with a Microfire CCD color camera (Optronics). Stereological analyses were performed using the Mercator software (Explora Nova, La Rochelle, France) and all cell counts were processed online on the video image. The same intensity of light in the microscope as well as the same parameters in the exposure time of the digital camera were used for all sections. For each section, areas of interest were first outlined using a × 2.5 objective (Figs. 3c, 4a), and c-Fos-positive neurons counting was performed using a ×100 (1.40 NA) oil-immersed objective (Figs. 3c, 4a). Randomly positioned grids (120 × 120 µm) containing counting frames (40 × 40 µm) equidistant from each other were superimposed in the area to be counted. For each animal, the estimated total number of c-Fos positive nuclei was calculated from the total number of nuclei counted in all optical dissectors. Parameters of the optical fractionator program were as follows: area of counting frame of grid = 40 × 40 µm, section interval = 240 µm, dissector height = 10 µm and guard zones = 2 µm each (the latter corresponding to upper and lower borders exclusions, mean section thickness was 14 µm). The coefficients of error reflect the variation in sampling within each animal and represent the estimated precision of the population size calculated by the optical fractionator (Gundersen et al. 1988); they ranged from 0.04 to 0.14.

Statistical analysis

Water maze acquisition data were analyzed using a three-way ANOVA with Lesion (ReRh *vs* Sham) and Delay (5 days vs 25 days) as between-subject factors, and day (1, 2… 8) as the repeated measure. Probe trial performance was analyzed using a two-way Group X Delay ANOVA. The time spent in the target quadrant during the probe trial was also compared to chance (i.e., 15 s) using a one-sample Student's t test. Data of spine densities were analyzed using a three-way ANOVA with the following factors: Learning (home cage vs learning), Lesion (Sham, ReRh), and Delay (5 vs 25 days) for each spine type. c-Fos quantification were analyzed the same way as spine density, using a three-way ANOVA for each structure (CA1, CA3, and DG for the dHip; IL, PL, and

ACC for the mPFC). When appropriate, post hoc analyses used a Newman–Keuls test. Occasionally, when a figure suggested possible differences, multiple comparisons were performed, even in the absence of a significant interaction, as advocated by Howell (1992). An effect or a difference was considered significant when $p < 0.05$.

Results of Experiment 1: Water maze learning, ReRh lesion and spine density in the dorsal hippocampus and prefrontal cortex

Location and extent of ReRh lesions

Figure 1B shows the largest and the smallest ReRh lesion along with photographs of tissue stained for NeuN. Quantification of the lesion extent (volume of damaged tissue) showed that there was, on average (±SEM), 74.0% (±3.0) damage to the Re, 29.7% (±3.6) to the left pRe, 35.5% (±4.0) to the right pRe, and 48.7% (±5.2) to the Rh. Damage to thalamic structures other than the ReRh or pRe ranged generally from non detectable to modest: the lesion encroached onto 24.1% (±3.6) of the submedian nucleus, and 7.6% (±1.8) of the anteromedian one. These lesions are comparable to those of our former studies (Ali et al. 2017; Loureiro et al. 2012). Incidental unilateral damage (due to cannula lowering into the brain) to overlying areas of the intralaminar and mediodorsal thalamic nuclei, dHip and cortex was of limited incidence.

After water maze learning, recent memory was operational but failed to persist in rats with ReRh lesion

Water maze performance is illustrated in Fig. 1c. When rats had to swim to a visible platform, we found no significant difference among groups on distances, latencies, thigmotaxis, and swimming speed; only a significant overall Trial effect was noticed on distances and latencies, both of which became shorter over trials ($F_{3,105} = 85.6$, $p < 0.001$). The ANOVA of the distances to reach the hidden platform during the acquisition phase of the task only showed a significant day effect ($F_{7,245} = 25.3$, $p < 0.001$), reflecting learning. The absence of significant Lesion ($F_{1,35} = 0.5$, NS) and Delay ($F_{1,35} = 2.8$, NS) effects, and the fact that none of the interactions was significant indicated that the learning curves were not different among experimental groups. Thus, performance during task acquisition was not affected by the ReRh lesion. The ANOVA of the latencies confirmed all observations made on distances, and both thigmotaxis and swimming speeds were similar among groups (data not shown). On probe trial performance (i.e., time in the target quadrant), the ANOVA showed a significant Lesion ($F_{1,35} = 9.002$, $p < 0.01$) and a significant delay ($F_{1,35} = 21{,}451$, $p < 0.001$) effect, but no significant interaction between the two factors. It is noteworthy, however, that when the time in the target quadrant was compared to chance (i.e., 15 s) within each group, Sham rats performed significanlty above chance at both delays ($p < 0.01$); at the 25-day delay, performance of ReRh rats did not differ from chance ($p = 0.664$). Thus, 25 days after learning, ReRh rats had forgotten the location of the platform, confirming our former study (Loureiro et al. 2012). In contrast with our previous studies (e.g., Ali et al. 2017; Loureiro et al. 2012), we found that ReRh exhibited a weak but significant deficit after five post-acquisition days. It is to note, however, that, at this delay, these rats performed significantly above chance ($p < 0.01$), indicating that they remembered the platform location. Multiple comparisons also showed a significant difference between ReRh rats tested 5 days after acquisition compared to rats tested after 25 days ($p < 0.01$).

Spine density in the dorsal hippocampus

Typical examples of spines are shown in Fig. 2a. The most significant quantitative data are illustrated in Fig. 2c. All other data are presented in Tables 1 and 2. Intra-subject variability of spine density was observed, whether on mushroom or thin or stubby spines, sometimes following group mean fluctuations, sometimes not. For mushroom spines, the overall average intra-subject SEM reached between 16 (CA1) and 25% (CA3) of the mean value in each subregion of the hippocampus. For thin and stubby spines, the overall average SEM reached between 4.5 (DG) and 7.4% (CA3) of the mean value. There was no evidence for a consistent lesion-mediated, learning-mediated or delay-mediated effect on variability, or of any of the interactions.

In CA3 and the dentate gyrus of the dorsal hippocampus, the number of thin and stubby spines was not modified by water maze learning or post-learning delay, but moderately altered by ReRh lesion

Data are shown in Table 1. The ANOVA of the number of thin and stubby spines counted on apical dendrites of region CA3 showed no significant effects of Learning ($F_{1,39} = 1.3$, NS), Lesion ($F_{1,39} = 0.7$, NS), or Delay ($F_{1,39} = 1.66$, NS). None of the interactions was significant. The same was found on basal dendrites (Learning: $F_{1,39} = 0.1$, NS; Lesion $F_{1,39} = 1.3$, NS; Delay: $F_{1,39} = 0.2$, NS). On apical dendrites of the dentate gyrus, we found a significant Lesion effect ($F_{1,39} = 7.9$, $p < 0.01$), due to a slightly larger overall number of spines in HC rats with an ReRh lesion. None of the interactions was significant.

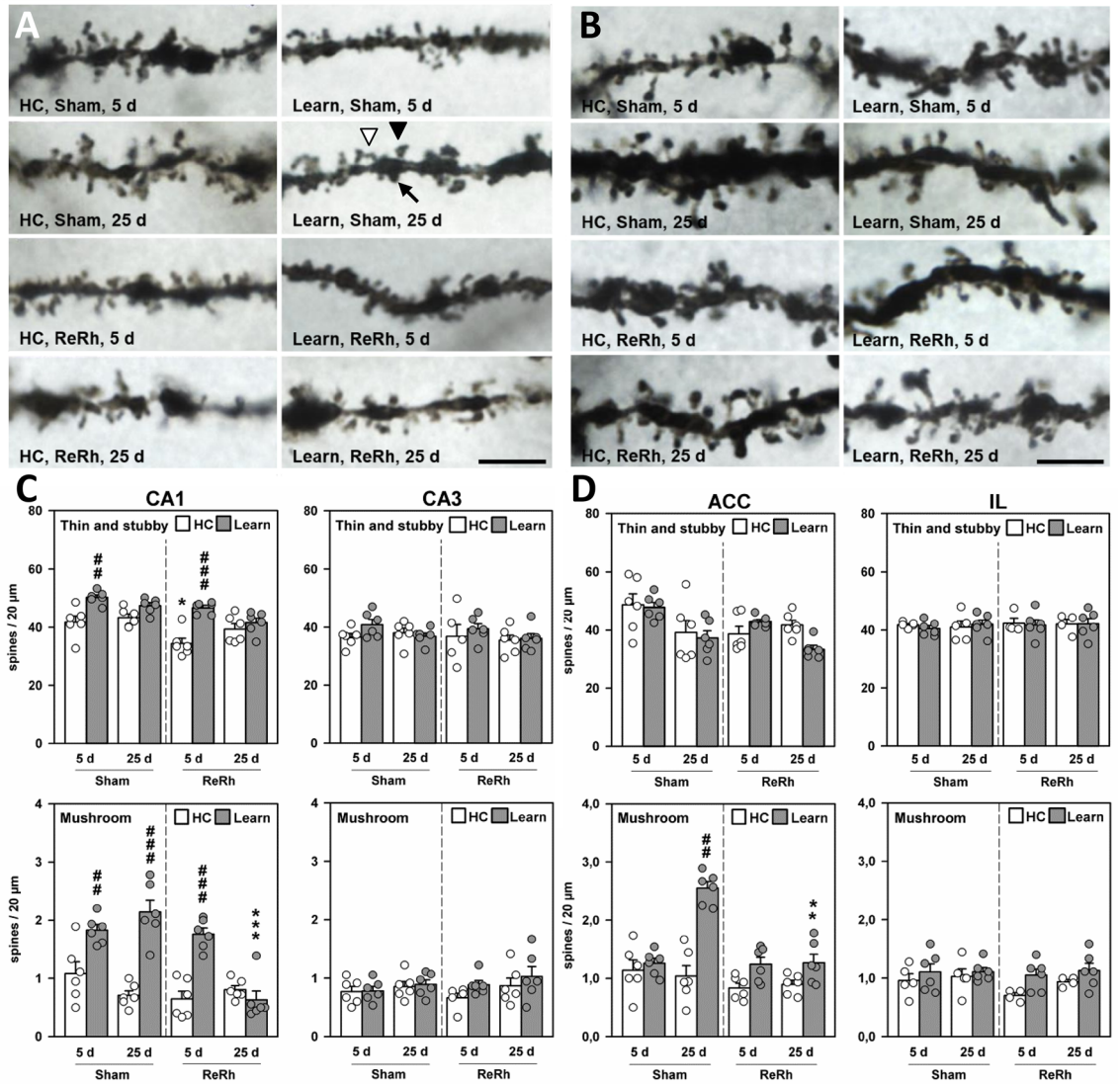

Fig. 2 **a** Dendritic spines in the dorsal hippocampus in Experiment 1. Photomicrographs showing typical examples of dendritic spines on apical dendrites in CA1 of control rats (HC for home cage) and rats that were trained (Learn) in the water maze and subsequently tested in a probe trial 5 or 25 days post-acquisition after a sham-operation (Sham) or a lesion of the reuniens and rhomboid (ReRh) nuclei. In the photograph labelled 'Learn, Sham, 25 days', the white arrow head shows a thin spine, the black arrow head shows a mushroom spine, and the regular black arrow points to a stubby spine. **b** Dendritic spines in the medial prefrontal cortex. Photomicrographs showing typical examples of dendritic spines on apical dendrites in the ACC of control rats (HC) and rats trained and tested in the water maze (Learn) after a sham-operation (Sham) or a lesion of the reuniens and rhomboid (ReRh) nuclei. Scale bar in A and B = 2 µm. **c** Spine density in the dorsal hippocampus. Average spine densities on apical dendrites in regions CA1 and CA3 of the dorsal hippocampus of rats that were trained (Learn) or not (HC) in a water maze task and subsequently tested in a probe trial 5 days (5 days) or 25 days (25 days) after the end of learning. Before training, rats had either been sham-operated (Sham) or subjected to an excitotoxic lesion of the reuniens and rhomboid nuclei (ReRh). In CA3, there were no significant modifications related to learning, lesion, or delay, whatever the type of spines considered (thin, stubby, or mushroom). On CA1 apical dendrites, after the 5-day delay, learning triggered an increase of thin and stubby spine density in both Sham and ReRh animals, a modification no longer observed after 25 days. On CA1 apical dendrites of Sham rats, learning triggered an increase in mushroom spine density after both post-acquisition delays. Rats with ReRh lesions showed a comparable change after the shortest delay (5 days); however, after 25 days, the spine density in ReRh animals returned to the baseline (i.e., HC controls) level, indicating that the plasticity triggered by learning did not last following ReRh lesions. Statistical analyses: significant effect of Learning: $^{\#\#}p < 0.01$, $^{\#\#\#}p < 0.001$; significant effect of Lesion: $^{*}p < 0.05$, $^{***}p < 0.001$. **d** Spine density in the medial prefrontal cortex. Average spine densities on apical dendrites in the anterior cingulate cortex (ACC) and infralimbic cortex (IL) cortices in the same rats as in **c**. In the IL, there were no significant modifications related to learning, lesion, or delay. On ACC apical dendrites of Sham rats, there was no effect of learning, lesion, or delay on thin and stubby spine density. However, learning triggered a marked increase in mushroom spine density at the 25 days post-acquisition delay. In ReRh rats, this modification was not detected, a difference that could account for impaired remote memory in ReRh rats. Statistical analyses: significant effect of Learning: $^{\#\#}p < 0.01$; significant effect of Lesion: $^{**}p < 0.001$

Table 1 Average (±SEM) number of thin and stubby dendritic spines/20 µm segment counted in the three subregions of the medial prefrontal cortex (mPFC) and of the dorsal hippocampus (dHIP) on apical or basal dendrites of rats subjected to sham operations (Sham) or ReRh lesions

Region	Dendrite	Surgery	HC 5 days	HC 25 days	Learn 5 days	Learn 25 days
mPFC	Apical	Sham	41.7 ± 0.4	40.9 ± 2.1	40.5 ± 1.0	41.9 ± 1.4
IL		ReRh	42.3 ± 1.7	42.0 ± 1.6	41.7 ± 1.8	42.1 ± 1.8
	Basal	Sham	39.6 ± 0.5	39.1 ± 0.7	38.3 ± 1.3	39.8 ± 1.3
		ReRh	42.8 ± 1.9	40.6 ± 2.4	40.2 ± 1.7	39.3 ± 0.9
PL	Apical	Sham	47.8 ± 0.9	48.6 ± 1.4	48.7 ± 1.5	48.8 ± 1.7
		ReRh	36.9 ± 1.3*	45.8 ± 0.6	50.1 ± 2.5#	49.8 ± 2.1
	Basal	Sham	47.5 ± 1.2	46.5 ± 2.1	48.3 ± 1.1	48.6 ± 1.1
		ReRh	38.2 ± 1.5*	44.6 ± 1.3	47.6 ± 1.8#	50.0 ± 2.0
ACC	Apical	Sham	48.6 ± 3.8	39.2 ± 4.1	47.7 ± 1.7	37.3 ± 2.5
		ReRh	38.7 ± 2.5	41.7 ± 1.6	42.8 ± 0.8	33.4 ± 1.3
	Basal	Sham	45.0 ± 3.7	37.6 ± 4.8	44.9 ± 2.8	36.2 ± 2.4
		ReRh	37.4 ± 2.2	40.1 ± 1.2	37.4 ± 0.6	29.3 ± 1.3
dHIP	Apical	Sham	36.5 ± 1.3	38.0 ± 1.6	40.8 ± 1.8	36.9 ± 1.1
CA3		ReRh	36.8 ± 4.1	35.4 ± 1.8	39.4 ± 1.8	36.1 ± 1.7
	Basal	Sham	33.4 ± 1.3	36.9 ± 2.2	36.1 ± 2.4	34.2 ± 1.3
		ReRh	33.4 ± 2.8	35.0 ± 1.3	33.8 ± 1.2	32.8 ± 0.9
DG	Apical	Sham	32.7 ± 1.8	34.1 ± 1.2	34.7 ± 1.5	33.7 ± 0.9
		ReRh	38.3 ± 1.8	39.0 ± 1.3	35.3 ± 2.2	35.2 ± 1.4
CA1	Apical	Sham	41.7 ± 2.1	43.3 ± 1.3	50.2 ± 0.9#	47.3 ± 1.1
		ReRh	34.4 ± 1.8*	39.3 ± 1.9	46.6 ± 0.8#	41.5 ± 1.5
	Basal	Sham	39.7 ± 2.1	39.5 ± 1.2	45.1 ± 1.2	42.7 ± 1.5
		ReRh	32.1 ± 1.7*	35.4 ± 1.9	42.4 ± 1.2#	38.1 ± 1.1

The rats were kept in their home cage (HC) or trained in a water maze task and subsequently tested for retention either 5 or 25 days following the end of acquisition (Learn). Statistics: *significant Lesion effect (vs. Sham at the same delay), $p < 0.05$; #significant Learning effect (vs. HC at the same delay), $p < 0.05$

In CA3 and the dentate gyrus of the dorsal hippocampus, the number of mushroom spines was not modified by water maze learning or post-learning delay, but there was a moderate ReRh lesion effect

For CA3, the data are illustrated in Fig. 2c. For the dentate gyrus, they are presented in Table 2. The ANOVA of the number of mushroom spines counted on apical dendrites of region CA3 showed no significant effects of Learning ($F_{1,34} = 2.2$, NS), Lesion ($F_{1,34} = 0.3$, NS) or Delay ($F_{1,34} = 3.4$, NS). None of the interactions was significant, indicating that the spine density was affected by none of the three variables. The same was true for apical spine density in the dentate gyrus, except that there was a significant overall Learning effect ($F_{1,39} = 15.8$, $p < 0.0005$), which was due to higher spine density in learners vs. baseline (home cage) rats. On basal dendrites of CA3 (see Table 2), none of the main effects and none of the interactions was significant.

In CA1 of the dorsal hippocampus, the number of thin and stubby spines was increased by water maze learning, but ReRh lesion and post-learning delay had no effects

The data are illustrated in Fig. 2c and Table 1. The ANOVA of the number of thin and stubby spines counted on apical dendrites of region CA1 showed significant effects of Learning ($F_{1,40} = 40.9$, $p < 0.001$) and Lesion ($F_{1,40} = 24.0$, $p < 0.001$), but not of Delay ($F_{1,40} < 1.0$, NS). The Learning × Delay interaction was also significant ($F_{1,40} = 11.9$, $p < 0.005$). All other interactions were not significant. Globally, learning increased spine density, but only at the shortest delay. ANOVA of thin and stubby spine density on the basal dendrites of region CA1 yielded similar main effects, interactions, and post hoc differences.

Table 2 Average (±SEM) number of mushroom dendritic spines/20 µm segment counted in the three subregions of the medial prefrontal cortex (mPFC) and of the dorsal hippocampus (dHIP) on apical or basal dendrites of rats subjected to sham operations (Sham) or ReRh lesions. The rats were kept in their home cage (HC) or trained in a water maze task and subsequently tested for retention either 5 or 25 days following the end of acquisition (Learn)

Region	Dendrite	Surgery	HC 5 days	HC 25 days	Learn 5 days	Learn 25 days
mPFC IL	Apical	Sham	0.96 ± 0.12	1.03 ± 0.13	1.11 ± 0.14	1.11 ± 0.07
		ReRh	0.70 ± 0.05	0.94 ± 0.04	1.05 ± 0.10	1.13 ± 0.12
	Basal	Sham	1.22 ± 0.15	1.00 ± 0.22	0.93 ± 0.04	1.10 ± 0.07
		ReRh	0.73 ± 0.14	0.72 ± 0.12	1.03 ± 0.11	1.17 ± 0.11
PL	Apical	Sham	1.35 ± 0.13	0.85 ± 0.11	1.27 ± 0.13	1.10 ± 0.12
		ReRh	0.74 ± 0.06*	0.84 ± 0.10	1.41 ± 0.15#	1.14 ± 0.19
	Basal	Sham	1.45 ± 0.11	0.96 ± 0.11	1.64 ± 0.19	0.88 ± 0.12
		ReRh	0.85 ± 0.16*	1.04 ± 0.06	1.35 ± 0.13	0.96 ± 0.08
ACC	Apical	Sham	1.14 ± 0.17	1.04 ± 0.18	1.26 ± 0.08	2.55 ± 0.11#
		ReRh	0.84 ± 0.08	0.90 ± 0.07	1.24 ± 0.12	1.27 ± 0.15*
	Basal	Sham	1.05 ± 0.12	0.86 ± 0.15	1.08 ± 0.09	2.08 ± 0.21#
		ReRh	0.78 ± 0.07	0.77 ± 0.14	1.01 ± 0.06	1.08 ± 0.21*
dHIP CA3	Apical	Sham	0.77 ± 0.09	0.86 ± 0.09	0.78 ± 0.07	0.89 ± 0.08
		ReRh	0.66 ± 0.09	0.87 ± 0.13	0.89 ± 0.07	1.03 ± 0.17
	Basal	Sham	0.83 ± 0.08	0.81 ± 0.08	0.63 ± 0.04	1.00 ± 0.18
		ReRh	0.60 ± 0.04	0.89 ± 0.13	0.91 ± 0.10	1.00 ± 0.09
DG	Apical	Sham	0.86 ± 0.16	0.57 ± 0.11	1.04 ± 0.15	1.22 ± 0.29
		ReRh	0.63 ± 0.06	0.74 ± 0.06	1.09 ± 0.11	1.21 ± 0.15
CA1	Apical	Sham	1.09 ± 0.20	0.71 ± 0.08	1.83 ± 0.10#	2.14 ± 0.20#
		ReRh	0.65 ± 0.13	0.81 ± 0.07	1.76 ± 0.11#	0.63 ± 0.15*
	Basal	Sham	0.58 ± 0.09	0.59 ± 0.08	1.26 ± 0.07#	1.32 ± 0.22#
		ReRh	0.50 ± 0.07	0.57 ± 0.06	1.07 ± 0.10#	0.48 ± 0.10*

*Significant Lesion effect (vs. Sham at the same delay), $p < 0.05$; #significant Learning effect (vs. HC at the same delay), $p < 0.05$

In CA1 of the dorsal hippocampus, the number of mushroom spines was dramatically modified by water maze learning, ReRh lesion and post-learning delay

The data are illustrated in Fig. 2c and Table 2. The ANOVA of the number of mushroom spines counted on apical dendrites of region CA1 showed significant effects of Learning ($F_{1,40} = 63.0$, $p < 0.001$), Lesion ($F_{1,40} = 24.0$, $p < 0.001$), and Delay ($F_{1,40} = 7.0$, $p < 0.05$). The following interactions were also significant: Learning x Lesion ($F_{1,40} = 10.0$, $p < 0.005$), Lesion x Delay ($F_{1,40} = 5.3$, $p < 0.05$), and Learning × Lesion × Delay ($F_{1,40} = 25.5$, $p < 0.001$). Post-hoc comparisons showed that, globally, learning increased spine density, while the lesion decreased it, as did the delay. In fact, compared to baseline, the number of spines was increased in Sham rats at both delays (5 days: $p < 0.01$; 25 days: $p < 0.001$) and in ReRh rats only at the shortest delay ($p < 0.01$); at the 25-day delay, the number of spines was no longer different from baseline (home cage condition) in ReRh rats. ANOVA of mushroom spine density on the basal dendrites of region CA1 yielded similar main effects, interactions, and post hoc differences.

Spine density in the medial prefrontal cortex

Typical examples of spines are shown in Fig. 2b. The most significant quantitative data are illustrated in Fig. 2d. All other data are presented in Tables 1 and 2. As for the hippocampus, an intra-subject variability was noticed. For mushroom spines, the average intra-subject SEM reached between 18% (CCA) and 22% (PL) of the mean value in each subregion of the mPFC. For thin and stubby spines, the average SEM reached between 4.1% (CCA, 5-days), and 5.1% (CCA, but 25 days) percent of the mean value. There was no evidence for a consistent lesion-mediated, learning-mediated or delay-mediated effect on variability, or of any of the interactions.

In the infralimbic cortex, the number of thin and stubby spines was not modified by water maze learning, ReRh lesion, or post-learning delay

The data are illustrated in Fig. 2d. The ANOVA of the number of thin and stubby spines counted on apical dendrites showed no significant effects of Learning ($F_{1,34} = 0.0$, NS), Lesion ($F_{1,34} = 0.4$, NS), or Delay ($F_{1,34} = 0.0$, NS). None of the interactions was significant. On basal dendrites,

none of the main effects and none of the interactions were significant.

In the prelimbic cortex, the number of thin and stubby spines was modified by water maze learning, ReRh lesion, and post-learning delay

The data are shown in Table 1. The ANOVA of the number of thin and stubby spines counted on apical dendrites showed significant effects of Learning ($F_{1,40}=16.2$, $p < 0.001$), Lesion ($F_{1,40}=6.1$, $p < 0.05$), and Delay ($F_{1,40}=4.4$, $p < 0.05$). Furthermore, the Lesion x Learning ($F_{1,40}=12.5$, $p < 0.01$) and Learning × Delay ($F_{1,40}=4.7$, $p < 0.05$) interactions were significant. These interactions can be explained by the decrease in the number of spines in Home cage rats with ReRh lesions at the short but not at the long delay, and this decrease was compensated for by water maze training. On basal dendrites, there were significant effects of Learning ($F_{1,40}=15.8$, $p < 0.001$) and Lesion ($F_{1,40}=5.6$, $p < 0.05$), and of the Learning × Lesion interaction ($F_{1,40}=7.0$, $p < 0.05$). The interaction can be interpreted in the same way as for the apical dendrites.

In the anterior cingulate cortex, the number of thin and stubby spines was moderately modified by ReRh lesion and post-learning delay

The data are illustrated in Fig. 2d The ANOVA of the number of thin and stubby spines counted on apical dendrites showed significant effects of Lesion ($F_{1,40}=5.1$, $p < 0.05$) and Delay ($F_{1.40}=13.5$, $p < 0.001$). These effects were due to a smaller number of spines in rats with a ReRh lesion and to an overall decrease of these spines over time. None of the interactions was significant. On basal dendrites, there were also significant effects of Lesion ($F_{1,40}=6.5$, $p < 0.05$) and Delay ($F_{1,40}=7.9$, $p < 0.01$), but none of the interactions was significant. The main effects can be interpreted in the same way as for the apical dendrites.

In the infralimbic cortex, the number of mushroom spines was moderately modified by water maze learning

The data are illustrated in Fig. 2d. The ANOVA of the number of mushroom spines counted on apical dendrites only showed a significant effect of Learning ($F_{1,34}=6.1$, $p < 0.05$), which, overall, reflected a slightly larger number of spines in trained rats. None of the interactions was significant. On basal dendrites, there was only a significant Learning × Lesion interaction ($F_{1,34}=7.4$, $p < 0.05$). The interaction was due to a non significant lesion-induced decrease of the number of spines, which the learning compensated for. None of the main effects and no other interaction were significant.

In the prelimbic cortex, the number of mushroom spines was moderately modified by water maze learning, post-learning delay, and ReRh lesion

The data are shown in Table 2. The ANOVA of the number of mushroom spines counted on apical dendrites showed significant effects of Learning ($F_{1,40}=10.0$, $p < 0.01$), Delay ($F_{1,40}=5.4$, $p < 0.05$), and of the Learnning × Lesion interaction ($F_{1,40}=4.4$, $p < 0.05$). The Learning effect reflected a higher number of spines in trained rats, and the Delay effect a reduced number after the long delay. The interaction is due to a lesion-induced reduction of the spine number in Home cage rats at the shortest delay, which learning had compensated for. On basal dendrites, there were significant effects of Lesion ($F_{1,40}=4.3$, $p < 0.05$) and Delay ($F_{1,40}=16.1$, $p < 0.001$). The Learning × Delay ($F_{1,40}=5.4$, $p < 0.05$) and the Lesion × Delay interactions ($F_{1,40}=8.4$, $p < 0.01$) were significant and can be interpreted in the same way as for the apical dendrites.

In the anterior cingulate cortex, the number of mushroom spines was dramatically modified by water maze learning, post-learning delay, and ReRh lesion

The data are illustrated in Fig. 2d. The ANOVA of the number of mushroom spines counted on apical dendrites showed significant effects of Learning ($F_{1,40}=45.1$, $p < 0.001$), Lesion ($F_{1,40}=23.6$, $p < 0.001$), and Delay ($F_{1,40}=12.8$, $p <0.001$). Furthermore, all interactions among main factors were significant (e.g., Learning × Lesion × Delay: $F_{1,40}=15.9$, $p < 0.001$). The main effects and the interactions were essentially due to the fact that learning resulted in a huge increase of the number of spines in Sham rats at the long delay when compared with the shortest one ($p <0.01$), a modification that was not observed in rats with a ReRh lesion. On basal dendrites, statistical analyses led to comparable conclusions: all main effects were significant, and when the interactions were not, they tended towards significance (Learning × Lesion: $F_{1,40}=3.1$, $p= 0.08$; Lesion × Delay: $F_{1,40}=3.4$, $p = 0.07$).

Results of Experiment 2: ReRh lesion and c-Fos expression

Location and extent of ReRh lesions

Figure 3a shows the largest and the smallest ReRh lesion along with photographs of tissue stained for NeuN.

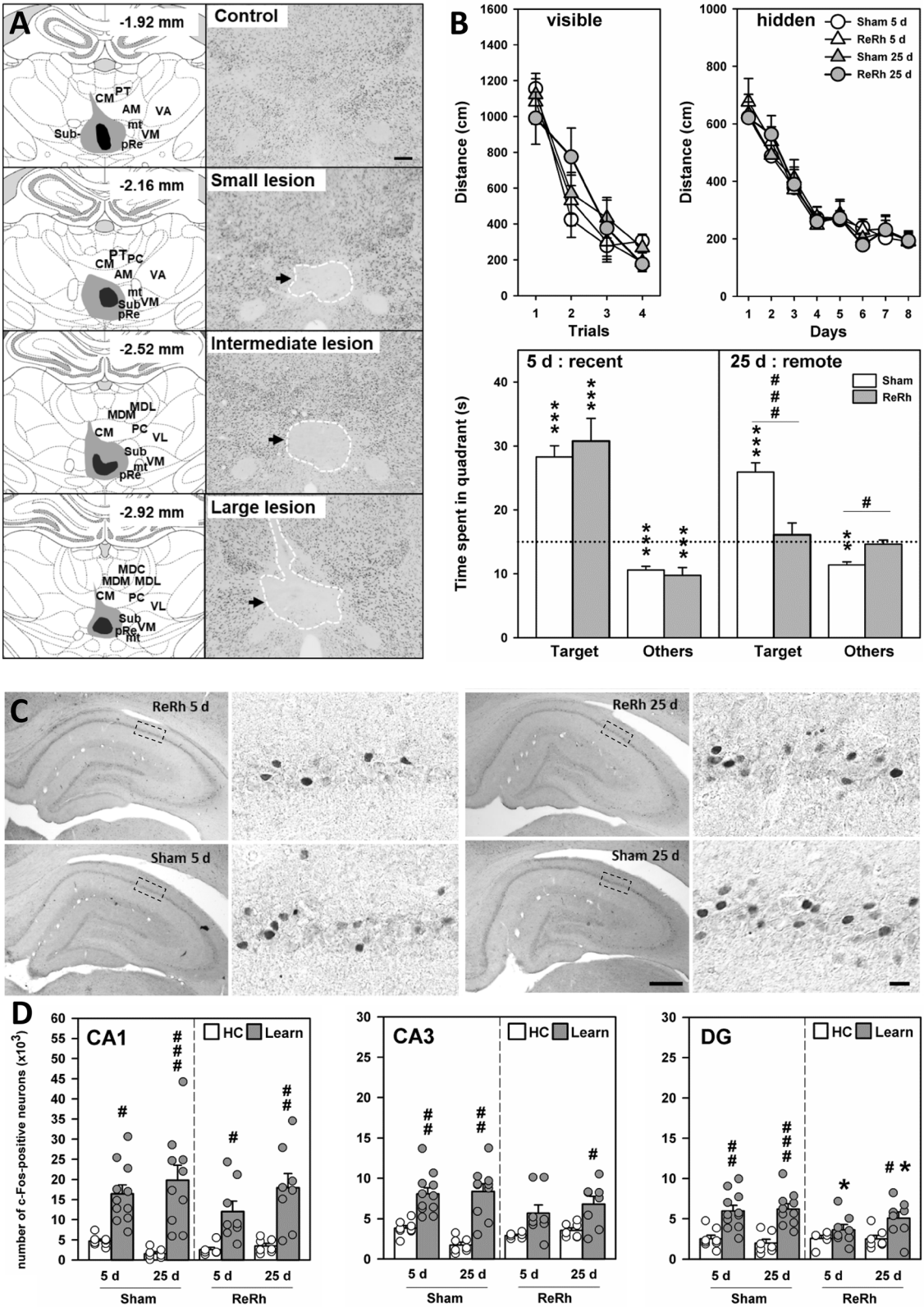

Quantification of the lesion extent (volume of damaged tissue) showed that there was, on average (±SEM), 71.9% (±2.4) damage to the Re, 45.1% (±4.8) to the left pRe, 40.4% (±3.6) to the right pRe, and 46,5% (±4.5) to the Rh. Damage to thalamic structures other than ReRh or pRe globally ranged from non detectable to modest: the lesion

◂**Fig. 3** **a** Lesion size and location (Experiment 2). Drawing of the smallest (dark gray) and largest (light gray) ReRh lesions (left) on coronal sections of the rat brain (anteroposterior level according to Paxinos and Watson 2007), and photomicrographs (right) illustrating some typical example of small and large lesions on brain sections immunostained for NeuN. Scale bar = 1 mm. Abbreviations: see caption of Fig. 1b. **b** Learning and memory performance in the water maze (WM) task. Performance of Sham and ReRh rats in the WM task with a visible platform (visible), with a hidden platform (hidden), and during the probe trial assessing recent memory at a post-acquisition delay of 5 days (5 days: recent), or remote memory after 25 days (25 days: remote). Confirming results of experiment 1 (Fig. 1c), the acquisition of the hidden platform location was similar in Sham and ReRh animals, and both groups remembered it at the 5-day delay, while at the 25-day delay, only sham-operated rats still remembered the platform location. Statistical analyses: significantly above chance level (dotted line): $^{**}p < 0.01$, $^{***}p < 0.001$; significant effect of the lesion: $^{\#}p < 0.05$. **c** Illustration of c-Fos immunohistochemistry in the dorsal hippocampus. Microphotographs illustrating typical c-Fos immunostaining in the hippocampus of Sham or ReRh rats tested in a probe trial either 5 days (5 days) or 25 days (25 days) after the end of the water maze task acquisition. For each microphotograph shown, a higher magnification of the region delimited by the stippled line is provided. Scale bar: small magnification = 500 µm; high magnification = 20 µm. **d** Stereological quantification of c-Fos-positive neurons in the dorsal hippocampus. Quantitative analysis of c-Fos-positive nuclei in CA1, CA3 and DG of the dorsal hippocampus after recent (5 days) or remote (25 days) memory retrieval (Learn) as compared to home cage (HC) control rats subjected to a sham-operation (Sham) or an excitotoxic lesion of the reuniens and rhomboid nuclei (ReRh). In rats with ReRh lesions, c-Fos expression was attenuated in the DG at both delays (recent and remote memory). In the two other areas, CA1 and CA3, no effect of the lesion was observed. Statistical analyses: significant effect of learning: $^{\#\#}p < 0.01$, $^{\#\#\#}p < 0.001$; significant effect of the lesion: $^{*}p < 0.05$, $^{***}p < 0.001$ (Newman–Keuls test)

encroached onto 13.6% (± 2.0) of the submedius nucleus, and 6.0% (± 1.9) of the anteromedial nucleus. These lesions are comparable with those of our former studies (Ali et al. 2017; Loureiro et al. 2012) and of our first experiment. Incidental unilateral damage (due to cannula lowering into the brain) to overlying areas of the intralaminar and mediodorsal thalamic nuclei, hippocampus, and cortex, was very limited.

Water maze learning and recent memory were normal, but memory did not persist in rats with ReRh lesion

Water maze performance is illustrated in Fig. 3b. When rats had to swim to a visible platform, we found no significant difference among groups on distances, latencies, thigmotaxis, and swimming speed. A significant overall Trial effect was noticed on distances (and on the other variables), which became shorter over trials ($F_{3,99} = 45.5$, $p < 0.001$). The ANOVA of the distances to reach the hidden platform during the acquisition phase of the task only showed a significant Day effect ($F_{7,231} = 58.5$, $p < 0.001$), which reflected learning. The absence of significant Lesion ($F_{1,33} = 0.1$, NS) and Delay ($F_{1,33} = 0.0$, NS) effects, and the fact that none of the interactions was significant indicated that the learning curves were not different among experimental groups. Thus, task acquisition was not affected by the ReRh lesion. The ANOVA of the latencies confirmed all observations made on distances; thigmotaxis, as well as swimming speeds, did not diverge among groups. On probe trial performance (i.e., time in the target quadrant), the ANOVA showed no significant overall Lesion effect ($F_{1,33} = 2.8$, NS). The Delay effect, however, was significant ($F_{1,33} = 15.2$, $p < 0.001$) as was the Lesion x Delay interaction ($F_{1,33} = 7.9$, $p < 0.01$). When the time in the target quadrant was compared to chance (i.e., 15 s) in each group, Sham rats performed significanlty above chance at both delays ($p < 0.01$), as did ReRh rats, but only at the 5-day delay ($p < 0.01$); at the 25-day delay, ReRh rats performed at chance level ($p = 0.582$). In other words, 25 days after learning, ReRh rats had forgotten the location of the platform, confirming our former study (Loureiro et al. 2012) and, herein, the findings of our first experiment.

Effects of ReRh lesion on c-Fos expression patterns after recent vs. remote memory retrieval

C-Fos expression was increased by learning in the dorsal hippocampus, and ReRh lesions slightly reduced it in CA3 and DG subfields

Typical c-Fos expression patterns are shown in Fig. 3c. The quantitative data are shown in Fig. 3d. The ANOVA of the number of c-Fos-positive neurons counted in the CA1 region only showed a significant effect of Learning ($F_{1,57} = 56.6$, $p < 0.001$). All other main effects and all interactions were not significant. Trained rats showed c-Fos expression levels that were dramatically increased (vs. their home cage controls). In the CA3 region, there was no significant effect of Lesion ($F_{1,57} = 0.7$, NS) or Delay ($F_{1,57} = 1.66$, NS), but the Learning effect was significant ($F_{1,57} = 56.9$, $p < 0.001$), reflecting increased numbers of c-Fos-positive neurons in trained rats. There was also a significant Lesion x Learning interaction ($F_{1,57} = 4.7$, $p < 0.05$). This interaction was due to the fact that following the ReRh lesion, the Learning effect was attenuated. All other interactions were not significant. Finally, in the dentate gyrus, there were no significant Lesion ($F_{1,57} = 2.6$, NS) or Delay ($F_{1,57} = 0.3$, NS) effects, but the Learning effect was significant ($F_{1,57} = 40.0$, $p < 0.001$); trained rats showed more c-Fos-positive neurons. There was also a significant Lesion × Learing interaction ($F_{1,57} = 5.1$, $p < 0.05$), which was due to a reduced effect of learning on the overall c-Fos expression level in ReRh rats as compared to their home-cage controls ($p < 0.01$).

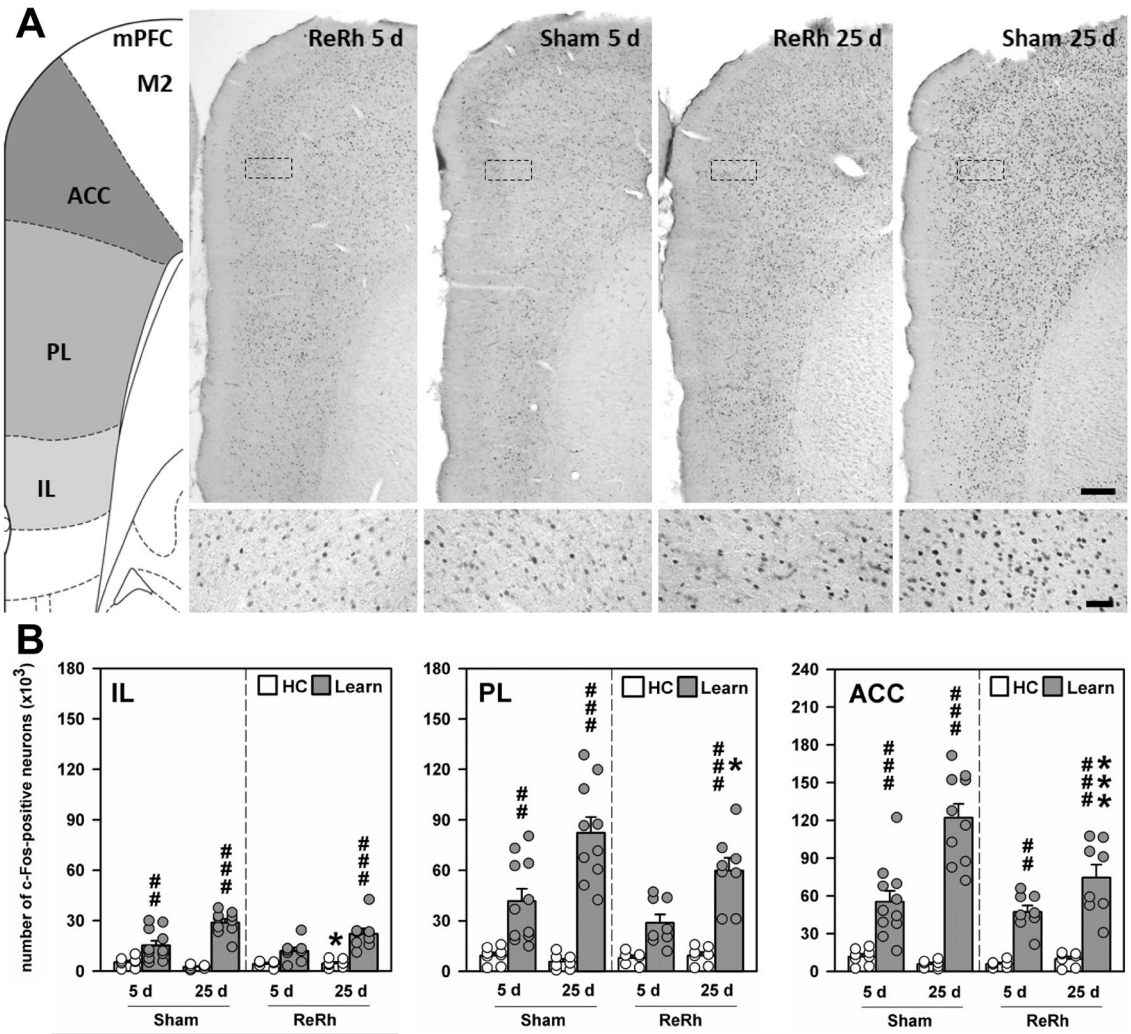

Fig. 4 **a** Illustration of c-Fos immunohistochemistry in the medial prefrontal cortex. Regions in which the quantifications were made are shown in the left panel according to Paxinos and Watson (2007), at Bregma + 3 mm (*ACC* anterior cingulate cortex, *PL* prelimbic cortex, *IL* infralimbic cortex). The other panels present microphotographs illustrating typical c-Fos immunostaining in the ACC of Sham or ReRh-lesioned rats which were tested in a probe trial either 5 days (5 d) or 25 days (25 d) after the end of the acquisition in the water maze task. The bottom band shows higher magnifications of the region delimited by a rectangle located in the ACC. Scale bar: smaller magnification = 500 µm; higher magnification = 50 µm. The increase in the number of c-Fos positive neurons observed in Sham rats at the 25-day delay was not observed in rats with ReRh lesions. **b** Stereological quantification of c-Fos-positive neurons in the medial prefrontal cortex. Quantitative analysis of c-Fos-positive nuclei in IL, PL and ACC of the mPFC after recent (5 days) or remote (25 days) memory retrieval (Learn) as compared to home cage (HC) control rats subjected to a sham-operation (Sham) or an excitotoxic lesion of the reuniens and rhomboid nuclei (ReRh). After a ReRh lesion, c-Fos expression was attenuated in PL and ACC at the longer delay (remote memory). Statistical analyses: significant effect of learning: $^{\#\#}p < 0.01$, $^{\#\#\#}p < 0.001$; significant effect of the lesion: $^{*}p < 0.05$, $^{***}p < 0.001$ (Newman–Keuls test)

C-Fos expression was increased by learning in the medial prefrontal cortex; the large potentiation of this effect by the post-learning delay was substantially reduced by the lesion

The data are illustrated in Fig. 4b. The ANOVA of the number of c-Fos-positive neurons counted in the infralimbic (IL) cortex showed significant effects of Learning ($F_{1,57} = 93.8$, $p < 0.001$) and Delay ($F_{1,57} = 11.1$, $p < 0.01$), not of Lesion ($F_{1,57} = 2.0$, NS). Overall, c-Fos expression levels were larger in trained (vs. home-cage) rats, and larger following remote (vs. recent) memory retrieval. There was also a significant Learning × Delay interaction ($F_{1,57} = 17.1$, $p < 0.001$), which was due to a number of c-Fos positive neurons that was larger after 25 days (vs. 5 days) in trained rats. In the prelimbic cortex (PL), the ANOVA showed significant effects of Learning ($F_{1,57} = 98.2$, $p < 0.001$) and Delay ($F_{1,57} = 14.5$, $p < 0.001$), not of Lesion ($F_{1,57} = 3.3$,

$p = 0.07$). Overall, c-Fos expression levels were larger in trained (vs. home-cage) rats, and larger following remote (vs. recent) memory retrieval. The Lesion × Learning ($F_{1,57} = 4.3$, $p < 0.05$) and Delay × Learning ($F_{1,57} = 16,5$, $p < 0.001$) interactions were the only significant interactions. They mainly reflected a reduced Learning effect in rats with ReRh lesion and a larger Learning effect at the 25 days (vs. 5 days) delay. Finally, in the ACC, the ANOVA showed significant Lesion ($F_{1,57} = 6,7$, $p < 0.01$), Learning ($F_{1,57} = 145.6$, $p < 0.001$) and Delay ($F_{1,57} = 17.3$, $p < 0.001$) effects. The main effects were due to c-Fos expression which was lower after the lesion (vs. Sham), higher after Learning (vs. home cage), and larger for remote (vs. recent) memory retrieval. There also were significant Lesion × Learning ($F_{1,57} = 5.9$, $p < 0.05$), Delay × Learning ($F_{1,57} = 19.0$, $p < 0.001$), and Lesion × Learning × Delay ($F_{1,57} = 5.0$, $p < 0.05$) interactions. The latter interaction was mainly due to a much reduced Learning effect in the rats with ReRh after the 25 days delay (vs. Sham at the same delay).

Discussion

After a ReRh lesion, rats acquired the water maze task, remembered it for at least 5 days (although exhibiting impaired performance when compared to their delay-matched controls), but performed at chance after 25 days (Loureiro et al. 2012). Because ReRh reversible inactivation did not hinder remote memory retrieval in a previous study of ours (Loureiro et al. 2012), we hypothesized that the ReRh lesion may have interfered with plasticity mechanisms underlying systems consolidation. Spatial learning resulted in an increased number of mushroom spines in the CA1 of Sham and ReRh rats. This increase persisted between 5 and 25 days post-acquistion in Sham rats, not in ReRh rats. In the ACC, learning increased the density of mushroom spines after 25 post-acquisition days in Sham rats, not in ReRh rats. Thus, ReRh lesions prevented the persistence of the increase of mushroom spines in CA1, and prevented subsequent learning-related spinogenesis in the ACC. We, therefore, hypothesized that if these lesion-induced effects underlined the absence of systems consolidation, rats with ReRh lesions, as opposed to their Sham-operated counterparts, should exhibit evidence for weaker activation in CA1 and/or ACC during remote memory retrieval. The c-Fos expression in the CA1 of ReRh rats was normal, for both recent and remote memory. However, in the ACC and PL, c-Fos expression was significantly reduced in rats with a ReRh lesion at the 25-day post-acquisition test.

This is the first of our ReRh studies in which, despite a significant recall of the platform position (time in target quadrant was significantly above chance level), we observed a reduction of performance at the 5-day post-acquisition delay in ReRh as compared to Sham rats. This reduction could reflect non-mnemonic effects of the lesions, as described earlier and discussed in terms of deficits in strategy shifting/behavioral flexibility. Indeed, in a water maze probe trial, rats with ReRh lesions were found to abandon searching for the platform earlier than their intact controls (Cholvin et al. 2013; Dolleman-van der Weel et al. 2009). This strategy shifting deficit could be due to a loss of excitatory inputs to mPFC (Dolleman-van der Weel et al. 2009), whereby inhibitory response control mechanisms could have been affected. However, we have no direct experimental evidence in favor of this possibility. Alternatively, an abnormally high performance level in our Sham rats was observed at the 5-day delay. Indeed, in our former experiment (Loureiro et al. 2012), the time Sham rats had spent in the target quadrant during the probe trial taxing recent memory was of 23 s in average, and thus reached 38% of the probe trial duration, as in the ReRh rats of the current study tested 5 days post-acquisition. At the same delay after exactly the same training protocol, Sham rats of the current experiment spent slightly more than 30 s (> 50%) in the target quadrant. Finally, it may be noteworthy that probe-trial performance were found to significantly exceed chance level in Sham rats at both delays and in ReRh rats at the 5-day delay. Thus, in these three groups, traces of the platform location appear operational as they permitted a targeted research of the platform during the probe trial. This was not the case in ReRh rats after 25 post-acquistion days.

Learning and time-dependent spine growth in the dorsal hippocampus and the mPFC

It is sometimes considered that thin or short spines are immature and unstable, whereas large spines are mature and stable, therefore, necessary for memory persistence (e.g., Bourne and Harris 2007; Kasai et al. 2010). Changes in hippocampal spine density after spatial learning have been described previously (e.g., Hongpaisan and Alkon 2007; Moser et al. 1994; O'Malley et al. 2000), although not always in terms of a learning-triggered increase (e.g., Ryan et al. 2015; Sanders et al. 2012). After spatial working memory training in a radial maze, Mahmmoud et al. (2015) found an increased spine density in the hippocampus of trained as compared to untrained cage controls rats. Restivo et al. (2009) documented time-dependent spine formation dynamics in the dHip and the ACC. 1 day after contextual fear conditioning, the number of spines in stratum radiatum (apical dendrites) and stratum oriens (basal dendrites) had increased in CA1. In layers II and III of the ACC, it was unchanged. Later (i.e., 30 days), the number of spines had decreased in CA1, but had increased in the ACC; such increase may extend over about 14 post-conditioning days

(Aceti et al. 2015). Similar results were reported by Abate et al. (2018), who showed an implication of Ephrin B2, a cell adhesion factor, in the dHip and mPFC plasticity underlying fear memory persistence in mice. Evidence that such cortical spinogenesis supports remote fear memory has also been provided (Cole et al. 2012; Vetere et al. 2011). As hippocampal lesions disrupted remote memory formation and spinogenesis in the mPFC, cortical plasticity underlying remote memory formation might be hippocampus-driven (Restivo et al. 2009).

At the time when remote contextual fear memory requires the mPFC, it no longer depends on the hippocampus (Frankland and Bontempi 2005). This is at variance with memories for locations. Indeed, recent spatial memory (assessed 5 days post-acquisition) depends on the dHip, not on the mPFC (Lopez et al. 2012), whereas remote spatial memory (assessed 25 days post-acquisition) is altered by reversible inactivation of either the ACC or the dHip, suggesting a systems consolidation process in which the memory is dependent on both structures. This finding is compatible with our following results: (i) water maze learning increased the number of mushroom spines in CA1 after five post-acquisition days, and this number did not decrease after 20 additional days; (ii) in CA1, there was an increased expression of c-Fos at both post-acquisition delays suggesting the contribution of the dHip to remote spatial memory recall; (iii) in the ACC, the number of mushroom spines had increased dramatically at the time of remote (not recent) memory testing, and (iv) c-Fos expression was more important for remote as compared to recent memory in the ACC (and the PL) of sham-operated rats. These data evidence show, for the first time, that spatial learning triggers a time- and region-dependent rearrangement of dendritic mushroom spines, which consists in a relatively rapid and persistent increase of spine density in region CA1 of the dHip, and a delayed increase in the ACC of the mPFC.

Thin and stubby spines also responded to learning, although more weakly than mushroom spines. Their density was significantly increased by learning, but only at the 5-day post-acquisition delay and only in the dHip. This indicates that thin and stubby spine density changes after recent memory formation and then, over time, returns to baseline. Thin and stubby spines are sometimes considered learning spines (e.g., Bourne and Harris 2007), and there is evidence in the literature indicating that thin spines can actually be increased after acquisition of a spatial task (e.g., González-Ramírez et al. 2014), or that their density may correlate with spatial memory performance (Harland et al. 2014; Pereira et al. 2014; Xu et al. 2017). In one study, thin and even stubby spines increased once water maze training was completed (Beltrán-Campos et al. 2011). Finally, it is noteworthy that treatments (aging, lesions…) that affect the density of mushroom spines also affect that of thin spines (e.g., González-Ramírez et al. 2014; Harland et al. 2014). Altogether, in line with previous findings (Lopez et al. 2012), our results in sham-operated rats indicate that recent spatial memory could be supported by connectivity changes in the CA1 regions of the dorsal hippocampus, which seemingly still contribute to remote memory when connectivity changes have also occured in the mPFC.

Effects of ReRh lesions on spine growth and spine persistence

ReRh lesions affect several cognitive processes engaging simultaneously the prefrontal cortex and the hippocampus. These processes include strategy shifting in a spatial navigation task (Cholvin et al. 2013), generalization of fear memory attributes (Xu and Südhof 2013), flexible adaptation of goal-directed behavior (Linley et al. 2016), and spatial working memory (Griffin 2015; Hembrook et al. 2012; Layfield et al. 2015; Maisson et al. 2018). ReRh lesions also interfere with systems consolidation by preventing the formation of a remote spatial memory while leaving acquisition and recent memory retrieval relatively undisturbed (Loureiro et al. 2012). Our present results provide new insight into the neurobiological causes of the non persistence of this memory. They combine at least two events: (i) the learning-triggered remodeling of hippocampal connections which did not persist between 5 and 25 post-acquisition days, and (ii) the time-dependent remodeling of cortical connections which did not occur in the mPFC (ACC) following ReRh lesions. That these alterations are causal to memory fading is not indisputable. It is noteworthy, however, that the rats in which remodeling of cortical connections was hindered by a ReRh lesion also exhibited a reduced c-Fos expression in the ACC and PL cortices after remote memory assessment, suggesting a reduced engagement of the mPFC during the probe trial. Conversely, c-Fos expression measured during recent memory retrieval in ReRh rats did not significantly differ from Sham control rats. The relationship between unchanged spine density in the mPFC after ReRh lesions and the remote memory deficit is further supported by data from the literature, although in a different task/species: because the transcription factor MEF2 (myocyte enhancer factor) negatively regulates spinogenesis, Vetere et al. (2011) increased its function in the ACC of mice by viral transfection shortly after contextual fear conditioning. When tested 7 days after the transfection, the mice exhibited evidence not only for reduced freezing towards context but also for disrupted spine growth, clearly indicating that the alteration of spinogenesis in the ACC hindered systems consolidation of memory. Our present results do not permit to attribute the absence of remote memory solely to the lack of spinogenesis in the ACC and PL. It is well possible that the combination

of this lack with the non persistant increase of spinogenesis in CA1 was in fact the determining reason. Indeed, reversible inactivation of one or the other of these two structures at a remote time point disrupted recall in a water maze probe trial (Lopez et al. 2012). Nevertheless, the fact that following a ReRh lesion a severe reduction of c-Fos expression was observed in the ACC of the mPFC after the probe trial is compatible with a higher incidence of the lesion-induced consequences on the reorganization of mPFC connectivity than on that of hippocampal connectivity. The fact that, during the remote probe trial, c-Fos expression was not reduced in the hippocampus of rats with ReRh lesions could be due to a new processing of the forgotten spatial context.

Conclusions

Our findings further support a role for the ReRh nuclei in systems consolidation and memory persistence. We have shown, for the first time in a very classical spatial memory task, that lesion of the ReRh disrupts two learning-triggered phenomena: persistence of remodeled hippocampal connections in CA1, and delayed spinogenesis in the mPFC. These alterations could explain the absence of systems-level consolidation of a spatial memory after ReRh lesions. Based on this, future studies could try to achieve a precise mechanistic idea of what the ReRh nuclei do for memory persistence. Relevant objectives encompass (i) the identification of the cell types (and their projection pattern) which, in the ReRh, are crucial to this consolidation, (ii) the understanding of how, at a molecular level, ReRh neurons regulate spine persistence and spinogenesis in the Hip and mPFC, respectively, and (iii) the characterization of the timing of the changes mediated by the ReRh nuclei during and after spatial learning.

Acknowledgements This work was supported by the Agence Nationale de la Recherche (ANR grant 14-CE13-0029-01), the University of Strasbourg, the CNRS, INSERM, and by the Région Alsace (a territory now belonging to *Région Grand Est*) which contributed (50%) to the PhD fellowship allocated to M.M.K. (the supplement was provided by the ANR, same grant as above), as well as by the French government which provided a PhD fellowship to T.C. The authors acknowledge Olivier Bildstein, Daniel Egesi and George Edomwony for their precious contribution to animal care, as well as Mathilde Köhler, Manon Gerum, and Martin Deligny for providing appreciable technical help. We also thank Ms Delphine Cochand for her proofreading of the manuscript.

Compliance with ethical standads

Conflicts of interest The authors declare no conflict of interest. The study conformed to the rules of the European Community council directive of 22 September 2010 (2010-63) and of the French Department of Agriculture. All approaches have been validated by a local ethical committee (CREMEAS - authorization n° AL/32/39/02/13). The ANR grant did not depend on any particular clause which might have influenced data collection, analysis, interpretation and reporting.

References

Abate G, Colazingari S, Accoto A, Conversi D, Bevilacqua A (2018) Dendritic spine density and EphrinB2 levels of hippocampal and anterior cingulate cortex neurons increase sequentially during formation of recent and remote fear memory in the mouse. Behav Brain Res 344:120–131

Aceti M, Vetere G, Novembre G, Restivo L, Ammassari-Teule M (2015) Progression of activity and structural changes in the anterior cingulate cortex during remote memory formation. Neurobiol Learn Mem 123:67–71

Ali M, Cholvin T, Muller MA, Cosquer B, Kelche C, Cassel JC, Pereira de Vasconcelos A (2017) Environmental enrichment enhances systems-level consolidation of a spatial memory after lesions of the ventral midline thalamus. Neurobiol Learn Mem 141:108–123

Beltrán-Campos V, Prado-Alcalá RA, León-Jacinto U, Aguilar-Vázquez A, Quirarte GL, Ramírez-Amaya V, Díaz-Cintra S (2011) Increase of mushroom spine density in CA1 apical dendrites produced by water maze training is prevented by ovariectomy. Brain Res 1369:119–130

Bourne J, Harris KM (2007) Do thin spines learn to be mushroom spines that remember? Curr Opin Neurobiol 17:381–386

Cassel JC, Pereira de Vasconcelos A, Loureiro M, Cholvin T, Dalrymple-Alford JC, Vertes RP (2013) The reuniens and rhomboid nuclei: neuroanatomy, electrophysiological characteristics and behavioral implications. Prog Neurobiol 111:34–52

Cholvin T, Loureiro M, Cassel R, Cosquer B, Geiger K, De Sa Nogueira D, Raingard H, Robelin L, Kelche C, Pereira de Vasconcelos A, Cassel JC (2013) The ventral midline thalamus contributes to strategy shifting in a memory task requiring both prefrontal cortical and hippocampal functions. J Neurosci 33:8772–8783

Cole CJ, Mercaldo V, Restivo L, Yiu AP, Sekeres MJ, Han JH, Vetere G, Pekar T, Ross PJ, Neve RL, Frankland PW, Josselyn SA (2012) MEF2 negatively regulates learning-induced structural plasticity and memory formation. Nat Neurosci 15:1255–1264

Dolleman-van der Weel MJ, Morris RG, Witter MP (2009) Neurotoxic lesions of the thalamic reuniens or mediodorsal nucleus in rats affect non-mnemonic aspects of watermaze learning. Brain Struct Funct 213(3):329–342

Frankland PW, Bontempi B (2005) The organization of recent and remote memories. Nat Rev Neurosci 6:119–130

González-Ramírez MM, Velázquez-Zamora DA, Olvera-Cortés ME, González-Burgos I (2014) Changes in the plastic properties of hippocampal dendritic spines underlie the attenuation of place learning in healthy aged rats. Neurobiol Learn Mem 109:94–103

Griffin AL (2015) Role of the thalamic nucleus reuniens in mediating interactions between the hippocampus and medial prefrontal cortex during spatial working memory. Front Syst Neurosci 9:29

Groenewegen HJ, Witter MP (2004) Thalamus. In: Paxinos G (ed) The Rat Nervous System. 3th ed

Gundersen HJ, Bagger P, Bendtsen TF, Evans SM, Korbo L, Marcussen N, Møller A, Nielsen K, Nyengaard JR, Pakkenberg B (1988) The new stereological tools: disector, fractionator, nucleator and point sampled intercepts and their use in pathological research and diagnosis. APMIS 96:857–881

Hallock HL, Wang A, Griffin AL (2016) Ventral midline thalamus is critical for hippocampal-prefrontal synchrony and spatial working memory. J Neurosci 36:8372–8389

Harland BC, Collings DA, Mcnaughton N, Abraham WC, Dalrymple-Alford JC (2014) Anterior thalamic lesions reduce spine density

in both hippocampal CA1 and retrosplenial cortex, but enrichment rescues CA1 spines only. Hippocampus 24:1232–1247
Hembrook JR, Onos KD, Mair RG (2012) Inactivation of ventral midline thalamus produces selective spatial delayed conditional discrimination impairment in the rat. Hippocampus 22:853–860
Hongpaisan J, Alkon DL (2007) A structural basis for enhancement of long-term associative memory in single dendritic spines regulated by PKC. Proc Natl Acad Sci USA 104:19571–19576
Hoover WB, Vertes RP (2012) Collateral projections from nucleus reuniens of thalamus to hippocampus and medial prefrontal cortex in the rat: a single and double retrograde fluorescent labeling study. Brain Struct Funct 217:191–209
Howell D (1992) Statistical methods for psychology. Duxbury Press, Belmont, p 338p
Kasai H, Fukuda M, Watanabe S, Hayashi-Takagi A, Noguchi J (2010) Structural dynamics of dendritic spines in memory and cognition. Trends Neurosci 33:121–129
Layfield DM, Patel M, Hallock H, Griffin AL (2015) Inactivation of the nucleus reuniens/rhomboid causes a delay-dependent impairment of spatial working memory. Neurobiol Learn Mem 125:163–167
Lesburgueres E, Gobbo OL, Alaux-Cantin S, Hambucken A, Trifilieff P, Bontempi B (2011) Early tagging of cortical networks is required for the formation of enduring associative memory. Science 331:924–928
Linley SB, Gallo MM, Vertes RP (2016) Lesions of the ventral midline thalamus produce deficits in reversal learning and attention on an odor texture set shifting task. Brain Res 1649:110–122
Lopez J, Herbeaux K, Cosquer B, Engeln M, Muller C, Lazarus C, Kelche C, Bontempi B, Cassel J-C, de Vasconcelos AP (2012) Context-dependent modulation of hippocampal and cortical recruitment during remote spatial memory retrieval. Hippocampus 22:827–841
Loureiro M, Cholvin T, Lopez J, Merienne N, Latreche A, Cosquer B, Geiger K, Kelche C, Cassel JC, Pereira de Vasconcelos A (2012) The ventral midline thalamus (reuniens and rhomboid nuclei) contributes to the persistence of spatial memory in rats. J Neurosci 32(29):9947–9959
Mahmmoud RR, Sase S, Aher YD, Sase A, Gröger M, Mokhtar M, Höger H, Lubec G (2015) Spatial and working memory is linked to spine density and mushroom spines. PloS One 10(10):e0139739
Maisson DJ, Gemzik ZM, Griffin AL (2018) Optogenetic suppression of the nucleus reuniens selectively impairs encoding during spatial working memory. Neurobiol Learn Memomry 155:78–85
Moser MB, Trommald M, Andersen P (1994) An increase in dendritic spine density on hippocampal CA1 pyramidal cells following spatial learning in adult rats suggests the formation of new synapses. Proc Natl Acad Sci USA 91:12673–12675
O'Malley A, O'Connell C, Murphy KJ, Regan CM (2000) Transient spine density increases in the mid-molecular layer of hippocampal dentate gyrus accompany consolidation of a spatial learning task in the rodent. Neuroscience 99:229–232
Paxinos G, Watson C (2007) The rat brain in stereotaxic coordinates, 6th edn. Academic Press/Elsevier, Amsterdam, Boston
Pereira AC, Lambert HK, Grossman YS, Dumitriu D, Waldman R, Jannetty SK, Calakos K, Janssen WG, McEwen BS, Morrison JH (2014) Glutamatergic regulation prevents hippocampal-dependent age-related cognitive decline through dendritic spine clustering. Proc Natl Acad Sci USA 111:18733–18738
Restivo L, Vetere G, Bontempi B, Ammassari-Teule M (2009) The formation of recent and remote memory is associated with time-dependent formation of dendritic spines in the hippocampus and anterior cingulate cortex. J Neurosci 29:8206–8214
Roy A, Svensson FP, Mazeh A, Kocsis B (2017) Prefrontal-hippocampal coupling by theta rhythm and by 2–5 Hz oscillation in the delta band: the role of the nucleus reuniens of the thalamus. Brain Structe Funct 222:2819–2830
Ryan TJ, Roy DS, Pignatelli M, Arons A, Tonegawa S (2015) Engram cells retain memory under retrograde amnesia. Science 348(6238):1007–1013
Sanders J, Cowansage K, Baumgärtel K, Mayford K (2012) Elimination of dendritic spines with long-term memory is specific to active circuits. J Neurosci 32(36):12570–12578
Squire LR, Genzel L, Wixted JT, Morris RG (2015) Memory Consolidation. Cold Spring Harbor Perspect Biol 7:a021766
Thielen JW, Takashima A, Rutters F, Tendolkar I, Fernández G (2015) Transient relay function of midline thalamic nuclei during long-term memory consolidation in humans. Learn Memory 22:527–531
Thierry AM, Gioanni Y, Dégénétais E, Glowinski J (2000) Hippocampo-prefrontal cortex pathway: anatomical and electrophysiological characteristics. Hippocampus 10:411–419
Varela C, Kumar S, Yang JY, Wilson MA (2014) Anatomical substrates for direct interactions between hippocampus, medial prefrontal cortex, and the thalamic nucleus reuniens. Brain Struct Funct 219:911–929
Vertes RP (2004) Differential projections of the infralimbic and prelimbic cortex in the Rat. Synapse 51:32–58
Vetere G, Restivo L, Cole CJ, Ross PJ, Ammassari-Teule M, Josselyn SA, Frankland PW (2011) Spine growth in the anterior cingulate cortex is necessary for the consolidation of contextual fear memory. Proc Natl Acad Sci USA 108:8456–8460
West MJ (2013) Getting started in stereology. Cold Spring Harbor Protoc 2013:287–297
West MJ, Slomianka L, Gundersen HJG (1991) Unbiased stereological estimation of the total number of neurons in the subdivisions of the rat hiuppocampus using the optical fractionator. Anat Rec 231:482–497
Xu W, Südhof TC (2013) A neural circuit for memory specificity and generalization. Science 339:1290–1295
Xu B, Sun A, He Y, Qian F, Liu L, Chen Y, Luo H (2017) Running-induced memory enhancement correlates with the preservation of thin spines in the hippocampal area CA1 of old C57BL/6 mice. Neurobiol Aging 52:106–116